

## Dislocation profile in cholesteric finger texture

T. Ishikawa and O. D. Lavrentovich

*Chemical Physics Interdisciplinary Program and Liquid Crystal Institute, Kent State University, Kent, Ohio, 44242*

(Received 26 July 1999)

The displacement field around an isolated elementary dislocation in a medium with one-dimensional periodicity is established experimentally. The system studied is a cholesteric fingerprint texture with a macroscopic ( $\sim 10 \mu\text{m}$ ) periodicity. The characteristic elastic length is smaller than the “interlayer” distance. As a result, the experimental dislocation profile deviates from the classic pattern predicted by the linear elastic theory but fits well with the recently suggested nonlinear theory of dislocation [Phys. Rev. E **59**, R4752 (1999)].  
[S1063-651X(99)51411-6]

PACS number(s): 61.30-v

### I. INTRODUCTION

Elementary topological defects in systems with broken translational symmetry are dislocations. Dislocations have been an object of intensive studies mainly in media with three-dimensional (3D) periodicity (solids) [1]. There are substantial differences between these classic dislocations and dislocations in media with reduced dimensionality of order, such as smectic, cholesteric, or hexagonal phases in liquid crystalline, polymer, and other soft-matter systems. These differences manifest themselves in dislocation profiles (configurations of the order parameter associated with the defect), dislocation self-energy, and interaction energy [2].

Despite numerous theoretical studies on dislocations in 1D periodic systems, see [2] and [3], experimental quantitative verification of their properties (most notably, the displacement field around the defect) is scarce. Maaloum *et al.* [4] used atomic force microscopy to study the free surface profile of a smectic copolymer domain deposited on a silicon wafer surface. Later, they developed a theory [5] of surface tension influence on the layer displacement in order to explain the observed profile. We present an experimental study on the dislocation profile in the bulk of a layered system [6]. The study is additionally motivated by a recent observation [7] that the classical linear theory does not describe properly the dislocation profile when the characteristic elastic length  $\lambda$  of the system is smaller than the period  $w$  of translational order.

As the system to study, we have chosen a cholesteric “fingerprint” texture with a period  $w \sim 10 \mu\text{m}$ . We briefly remind the reader that the cholesteric liquid crystal has a helicoid structure with local director rotating around a single axis with a period (pitch)  $P$  [8]. The fingerprint texture occurs when the cholesteric material is sandwiched between two plates that tend to align the helicoid axis in the plane of the cell. When viewed from above, the periodic director twist shows a fingerprintlike texture. The choice of this system for the dislocation studies is determined by two factors. First, displacements of layers at the micron scale can be easily visualized by optical microscopy. Second, the system is expected to satisfy the condition  $\lambda < w$  needed to verify the predictions of the nonlinear theory [7]. Really, the elastic length  $\lambda$  is determined to be  $\lambda = \sqrt{K/B}$ , where  $K$  and  $B$  are the effective curvature and compressibility moduli, respec-

tively. According to Lubensky-de Gennes coarse grained elastic theory of the cholesteric phase [8],  $K = 3K_{33}/8$  and  $B = K_{22}(2\pi/P)^2$ , where  $K_{33}$  and  $K_{22}$  are the bend and twist Frank constants, respectively. Thus,  $\lambda \sim (P/2\pi)\sqrt{3K_{33}/8K_{22}}$  is normally smaller than  $P$ .

### II. EXPERIMENT

The cholesteric fingerprint textures were created in flat cells bounded by two plates with homeotropic alignment layers that favor perpendicular orientation of the director  $\mathbf{n}$ . The homeotropic alignment does not impose in-plane torques on the fingerprint texture, which is an important factor simplifying the study of the dislocation profile. The glass plates were coated with the polymer JALS 217 (JSR Inc., Japan). Mylar films were used as spacers setting the cell thickness  $d = 14 \mu\text{m}$ . Nematic liquid crystal 4-n-pentyl-4'cyanobiphenyl was mixed with chiral dopant 4-(2-methylbutyl)-1-cyanobiphenyl to adjust the pitch  $P$  to  $14 \mu\text{m}$  so that  $d/P \sim 1$ . When the cell is filled with the cholesteric mixture, a fingerprint texture occurs with characteristic “stripes” oriented randomly in the plane of the cell. To align the stripe along one direction, the cell was placed between the poles of an electromagnet. With the in-plane magnetic field switched on, an electric field was applied across the cell in order to annul the initial random fingerprint texture by reorienting  $\mathbf{n}$  everywhere along the axis  $y$  normal to the plates. Once the electric field was turned off, the stripes grew parallel to the direction of the magnetic field. We controlled the amplitude of the magnetic field ( $\sim 0.5 \text{ T}$ ) so that the stripes grew very slowly ( $< 1 \mu\text{m/sec}$ ) until they occupied the entire cell. The procedure allows us to obtain well oriented stripe textures such as the one shown in Fig. 1(a). The size of the cell was large (1 inch square) compared to the stripe periodicity to reduce the edge effects and mimic the “bulk” behavior of dislocations. Most of the samples show very low dislocation density (less than one dislocation per  $\text{cm}^2$ ). We have observed only elementary dislocations so that the Burgers vector  $b = w$ . Note here that the actual periodicity  $w$  of the fingerprint textures is close to (and slightly larger than) the pitch  $P$  of the cholesteric helicoid ( $w \approx 15 \mu\text{m}$  while  $P \approx 14 \mu\text{m}$ ). In principle, the true periodicity of a nonperturbed cholesteric helicoid is  $P/2$ ; however, the bounding surfaces break the symmetry and establish a double period

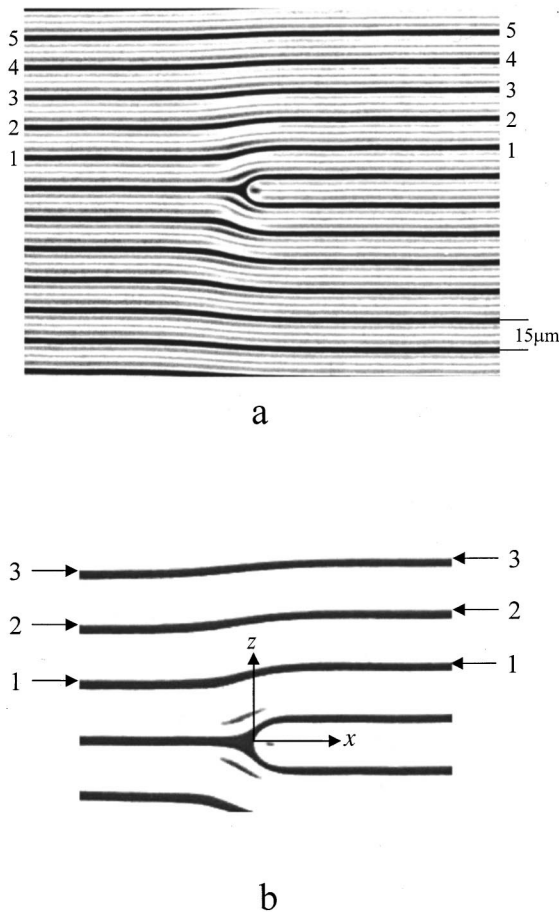


FIG. 1. (a) Typical appearance of the cholesteric stripe texture. (b) Location of the origin for profile measurements.

$w \approx P$  in the fingerprint textures, as discussed in [9].

Characterization of dislocations was performed with both magnetic and electric fields switched off. The stripe patterns around the dislocations were taken with a photographic camera attached to a polarizing microscope. The original images were expanded and traced on a large piece of paper. The accuracy in the determination of the stripes displacement is 0.4  $\mu\text{m}$ , determined mainly by the microscope's resolution. The location of the dislocation  $(x,z)=(0,0)$  was set at the tip of the semicircular end of the inserted layer; see Fig. 1(b).

### III. RESULTS AND DISCUSSION

Let us briefly describe the models of dislocation profile within the scope of linear [2,8] and nonlinear [7] elastic theories. As shown by Brener and Marchenko [7], the elastic energy density for a 1D layered system, accounting for the higher-order derivatives in the displacement field  $u(x,z)$  (nonlinear theory),

$$f = \frac{B}{2} \left\{ \frac{\partial u}{\partial z} - \frac{1}{2} \left( \frac{\partial u}{\partial x} \right)^2 \right\}^2 + \frac{K}{2} \left( \frac{\partial^2 u}{\partial x^2} \right)^2, \quad (1)$$

leads to the following dislocation profile:

$$u(x,z) = 2\lambda \ln \left[ 1 + \frac{e^{b/4\lambda} - 1}{2} \left\{ 1 + \operatorname{erf} \left( \frac{x}{2\sqrt{\lambda z}} \right) \right\} \right], \quad (2)$$

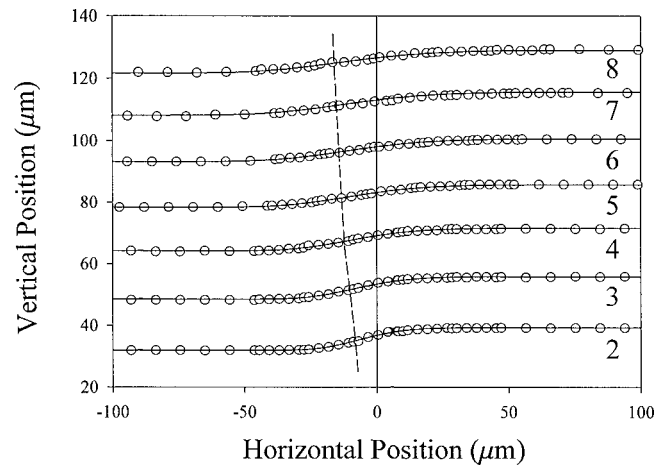


FIG. 2. Experimentally obtained profiles for the second through eighth layers. The dislocation lies at  $z=0$ . The fitting to nonlinear profiles is shown by the solid line. Experimental inflection points are marked by the dashed line.

where  $\operatorname{erf}(\dots)$  is the error function, the axis  $x$  is parallel to the layers (stripes), and the axis  $z$  is perpendicular to them. In the limit  $b \ll \lambda$ , Eq. (2) reduces to the result from the linear elastic theory [2,8],

$$u(x,z) = \frac{b}{4} \left\{ 1 + \operatorname{erf} \left( \frac{x}{2\sqrt{\lambda z}} \right) \right\}. \quad (3)$$

When  $b \sim \lambda$  or  $b > \lambda$ , the effect of nonlinearity has to be taken into account even at the large distance from the defects core.

Figure 2 shows the experimentally measured displacements of the second through eighth layers around the dislocation core. The displacement field was determined at a sharp border line between the dark and bright parts of the texture, indicated by arrows in Fig. 1(b). We will refer to these border lines as "layers" in what follows. The observed total displacement of a given layer (i.e., the difference in the  $z$  coordinate between the right and the left ends of the layer) slightly depends on the number of the layer: 7.8  $\mu\text{m}$  for the first layer, 7.6  $\mu\text{m}$  for the second, 7.5  $\mu\text{m}$  for the third, and 7.4  $\mu\text{m}$  for the fourth. Theoretically, the total displacement is half of the periodicity and should remain constant regardless of the distance from the dislocation core when the system is infinitely large. Although the small decrease in the total displacement might be easily attributed to the resolution of the optical patterns, it might also be indicative of the finite (although very large as compared to  $w$ ) size of our experimental cell. In the following, we disregard the first layer which is too close to the core region. The layers with numbers higher than 8 are of lesser interest since their displacements occur over larger distances (along the  $x$  axis) and the corresponding derivatives  $\partial u / \partial x$  are weak.

The main difference between the linear and nonlinear theories is the asymmetry of the dislocation profile. According to Eq. (3), the change in the displacement field mainly takes place in the range  $-\sqrt{\lambda z} < x < \sqrt{\lambda z}$ . In the linear theory, the point of inflection, where  $\partial^2 u / \partial x^2 = 0$ , is located at  $x=0$ . On the other hand, the nonlinear theory (2) predicts that the displacement is asymmetric, with the inflection point

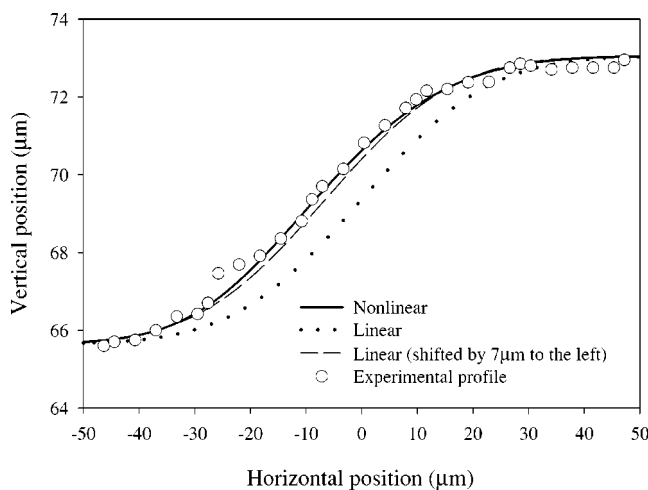


FIG. 3. Comparison between the measured and calculated profiles. See inset for details.

located at  $x < 0$ . The displacement changes mainly in the region of negative  $x$ , with the lower boundary being  $|x_{\min}| \sim \sqrt{bz} > \sqrt{\lambda z}$  [7]. This results in the effective shift of the displacement profile to the negative  $x$ 's and in the specific asymmetry: a sharp rise when  $x < 0$  and a slower saturation at  $x > 0$ .

Figure 3 shows the measured profile (circles) around the origin for the fourth layer. It is asymmetric: the larger part of the displacement ( $\sim 5.4 \mu\text{m}$  of the total  $7.4 \mu\text{m}$ ) takes place at  $x < 0$  and the inflection point is located at  $x = -7 \mu\text{m}$ . Figure 3 also shows the fitting to the nonlinear (2) and the linear (3) profiles with the same parameters  $b = 14.9 \mu\text{m}$  and  $\lambda = 2.65 \mu\text{m}$ . Evidently, the nonlinear model

fits the experimental data much better than the linear model. Moreover, the nonlinear theory with the very same pair of parameters  $b = 14.9 \mu\text{m}$  and  $\lambda = 2.65 \mu\text{m}$  fits nicely the whole set of profiles for all seven layers presented in Fig. 2.

It is expected that the differences between the linear and nonlinear descriptions will be significant only when  $\lambda \ll b$  [7]. In the system under study,  $\lambda$  is smaller than  $w = b$  only by a factor smaller than 10. One might thus wonder if it is possible to achieve a better agreement between the experimental data and the linear theory by readjusting the parameters of the fitting. Figure 3 suggests that a better fit might indeed be obtained by simply shifting the profile predicted by a linear theory to the left. However, the fit can be obtained only for one layer (layer number four in Fig. 3). If the same shift is applied to other layers, the linear theory does not fit the data at all. In contrast, the nonlinear theory fits all the layers with the same parameters  $b$  and  $\lambda$ , and with the same fixed origin at the core of the dislocation, Fig. 2. Therefore, the observed asymmetry in the displacement field is a real manifestation of the nonlinear elastic effects rather than an artifact associated with the setting of the origin for the profile measurement.

To conclude, we examined the displacement field of layers around an isolated elementary dislocation in cholesteric stripe textures. Experimental data are well described by a recently suggested nonlinear model of dislocation [7]. In particular, the nonlinear effects manifest themselves in the asymmetry of the dislocation profile.

#### ACKNOWLEDGMENT

The work was supported by the NSF Science and Technology Center ALCOM under Grant No. DMR89-21409.

- [1] J. Friedel, *Dislocations* (Pergamon Press, Oxford, 1964).
- [2] M. Kléman, *Points, Lines and Walls* (Wiley, New York, 1983).
- [3] R. Holyst and P. Oswald, Int. J. Mod. Phys. B **9**, 1515 (1995).
- [4] M. Maaloum, D. Ausserre, D. Chatenay, G. Coulon, and Y. Gallot, Phys. Rev. Lett. **68**, 1575 (1992).
- [5] M. S. Turner, M. Maaloum, D. Ausserre, J-F. Joanny, and M. Kunz, J. Phys. II **4**, 689 (1994).
- [6] We thank M. Kléman for illuminating consultations on the

available results about the dislocation structures. See also M. Kléman, Liq. Cryst. **3**, 1355 (1988) for the discussion of dislocations in materials with small and large layer rigidity.

- [7] E. A. Brener and V. I. Marchenko, Phys. Rev. E **59**, R4752 (1999).
- [8] P. G. de Gennes and J. Prost, *Physics of Liquid Crystals*, 2nd ed. (Clarendon Press, Oxford, 1992).
- [9] D. Subacius, S. V. Shiyanovskii, P. Bos, and O. D. Lavrentovich, Appl. Phys. Lett. **71**, 3323 (1997).